



The Frequency Distribution Estimation Method of Excess Rainfall Intensity of Double Thresholds (ERI_d) for Combined Sewer Overflow

Xingpo Liu¹ · Liang Shen¹ · Wenke Zang¹ · Yuwen Zhou²

Received: 11 January 2024 / Accepted: 22 April 2024 / Published online: 9 May 2024
© The Author(s), under exclusive licence to Springer Nature B.V. 2024

Abstract

Nowadays, many cities in China are facing the challenge of returning black and odorous waters during the rainy seasons. Combined sewer overflow (CSO) was one of the critical triggers. In this study, a new method for estimating frequency distribution of the excess rainfall intensity considering double thresholds (ERI_d in short) was proposed, which is helpful for estimating severity of CSO. For the specific interceptor well, the upper threshold is the design areal unit discharge (the equivalent rainfall intensity) of its upstream combined sewer and the lower one is the design areal unit discharge of its downstream interceptor sewers minus dry weather flow rate. First, rainfall events were divided and the minimum inter-event time (MIET) was set based on the time of concentration of the combined sewer catchment. Second, double-threshold method was used for ERI_d calculation and sampling for scenario of 30-minute CSO duration. Finally, the empirical frequency of the sampled $ERI_{d(30)}$ was calculated by the mathematical expectation formula (Weibull formula) and five functions (doubly censored exponential distribution, exponential function, Gumbel distribution, Weibull distribution and lognormal distribution) were used for comparison to obtain the best theoretical frequency distribution. Results revealed that: (1) The excess rainfall intensity of double thresholds (ERI_d) is suitable for characterizing CSO. (2) The frequency distribution of ERI_d was right (positively) skewed. (3) The kurtosis of the ERI_d samples is not greater than 3 for all the thresholds studied, which indicates that the distribution is thin-tailed. (4) The optimal frequency distribution function for ERI_d is doubly censored exponential distribution.

Highlights

- The double-threshold method of ERI was proposed for characterizing CSO.
- The frequency distribution is right (positively) skewed and thin-tailed.
- The doubly censored exponential distribution was the optimal one of ERI_d .

Keywords Combined Sewer Overflow (CSO) · Excess Rainfall Intensity of Double Thresholds (ERI_d) · The Combined Interceptor well · Return Period · The Doubly Censored Exponential Distribution

Abbreviations

CSO	Combined sewer overflow
CSS	Combined sewer system
Cs	Coefficient of skewness
Cv	Coefficient of variation
ERI _{d(30)}	Excess rainfall intensity of double thresholds (30 min)
MIET	The minimum inter-event time
MCMC	Markov Chain Monte Carlo
POT	Peak over threshold
SWMM	Storm water management model
WWTP	Wastewater treatment plant

1 Introduction

Combined sewer overflow (CSO) pollution was a challenge facing urban water environment managers across the globe (Atauzzaman et al. 2022; Campisano et al. 2016; Liu et al. 2023; Quaranta et al. 2022; Salam 2024). In China, many cities were haunted by the issue of returning black and odorous waters during the rainy seasons (Dai et al. 2020; Guan et al. 2023; Li et al. 2021; Pu et al. 2022; Wang et al. 2020) and CSO is one of the important causes of this issue. In this context, the demand for the effective control of CSO is becoming increasingly urgent.

For CSO pollution abatement, the fundamental questions are to study the rainfall intensity threshold and calculate the frequency (or return period) and volume of CSO. Three types of the relevant investigations were conducted in the past decade. The first type is to determine the critical rainfall intensity threshold that CSO may occur based on 16 years of CSO and precipitation data in Cumberland, Maryland, USA (Bizer et al. 2022). The second one is to predict the return period of CSO based on the multi-year rainfall records and empirical data of CSO outlets (Mailhot et al. 2015; Yu et al. 2013, 2018). The third one is to evaluate the performance of CSO facilities and assess the impact of climate change on CSO based on rainfall intensity thresholds (Andrés-Doménech et al. 2010; Fortier et al. 2015; Schroeder et al. 2011).

However, the above methods are all simulation driven (e.g. storm water management model (SWMM) or observed data-driven, and do not consider the physical mechanism of CSO occurrence, resulting in uncertainty of the calculation results. Hence, the low-return-period rainfall intensity formula was proposed to calculate the design discharge of the interceptor sewers and initially estimate the rainfall intensity threshold of CSO for the specific interceptor well (Liu et al. 2023). Meanwhile, the probability distribution of excess rainfall intensity (ERI) was investigated to estimate the volume of CSO based on POT (peak over threshold) sampling and the Generalized Pareto Distribution (GPD) (Liu et al. 2024). It only take one threshold (the lower threshold) of CSO into consideration. Physically, CSO volume from the specific interceptor well depends on the relationship between transfer flow rate of the upstream combined sewer and the interceptor flow rate of the downstream interceptor sewer, therefore CSO occurrence is a double-threshold phenomenon in essence. In this context, the concept of excess rainfall intensity of double thresholds (ERI_d in short) was proposed and its frequency distribution was investigated in this work.

The rest of this study is organized as follows: Sect. 2 details the rationale and flowchart of the proposed method. Section 2.1 describes the rainfall event division scheme. Section 2.2 illustrates the sampling method of ERI_d . Section 2.3 describes the method for calculating the empirical frequency of ERI_d . Section 2.4 describes the optimization method of the frequency distribution of ERI_d . Results of the case study are demonstrated in Sect. 3. Finally, findings of this work are summarized in Sect. 4.

2 Methodology and Data

Based on the recorded long-term rainfall series, the flowchart for the derivation of the frequency distribution model of ERI_d is presented in Fig. 1.

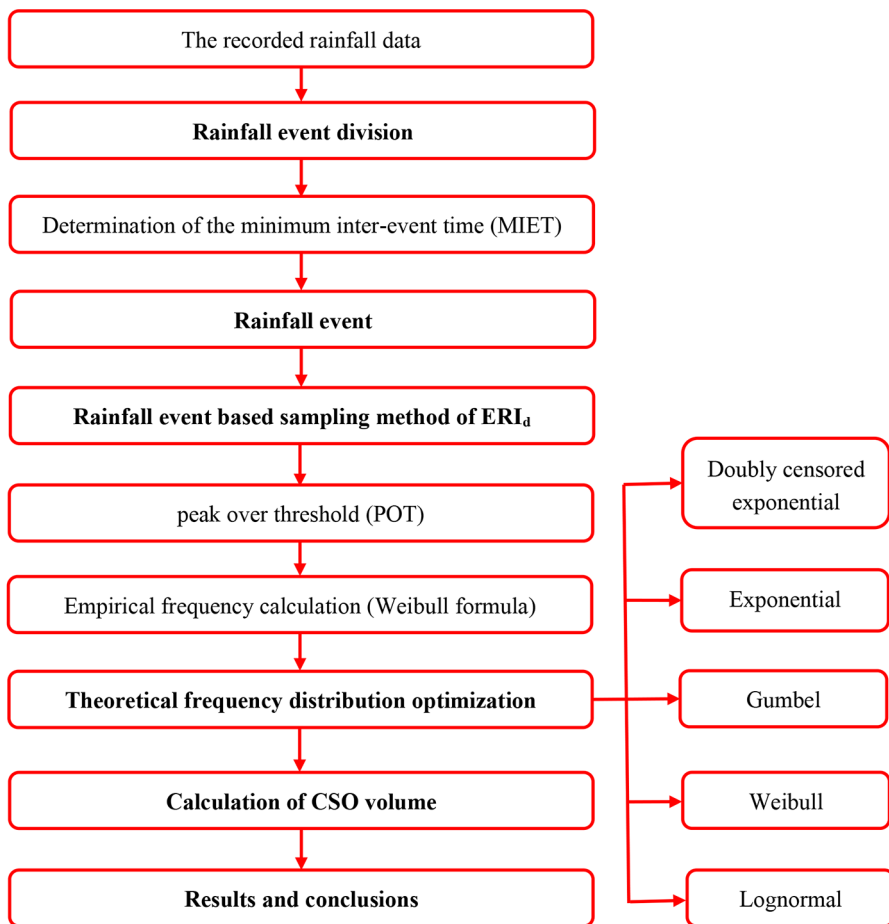


Fig. 1 Flowchart of this study

2.1 Rainfall Event Division Method

CSO events originate from rainfall events, and how rainfall events are divided is crucial to identify CSO events and calculate their frequency. The minimum inter-event time (MIET) is a key parameter for rainfall event division. For CSO scenario, MIET between two rainfall events should be greater than or equal to the time of concentration of the tributary area of the interceptor well studied (Liu et al. 2023). For urban catchments connected to a combined sewer system, the time of concentration normally does not exceed 2–3 h (Zhang et al. 2016). Rainfall statistical analysis software (RSAS) was developed to divide rainfall events in this study (Liu et al. 2023).

2.2 Sampling Method of ERI_d

As mentioned above, CSO occurrence is a double-threshold phenomenon. Here, the lower threshold is the design discharge of the downstream interceptor sewers minus the average dry weather flow(Liu et al. 2024), while the upper threshold is the design discharge of the upstream combined sewers. If the actual flow rate is larger than the upper one, the street flooding will occur. Otherwise, it will be discharged into the interceptor well (or sewer). The calculation principle of ERI_d was detailed in Fig. 2.

Among them, the design discharge of combined sewers can be obtained from the rainfall intensity formula (intensity-duration-frequency curve or IDF curve) while that of the interceptor sewers can be calculated from the low-return-period rainfall intensity formula (Liu et al. 2023), as shown in Fig. 3. The form of the above rainfall intensity formula in China was shown in Eq. (1).

$$i = \frac{A_1(1 + C \lg P)}{(t + b)^n} \tag{1}$$

where i is the rainfall intensity, P is the return period, t is the rainfall duration, and A_1, C, b, n are the local parameters of the specific city, which can be obtained by the maximum likelihood estimation method, Markov Chain Monte Carlo (MCMC) method, and so on.

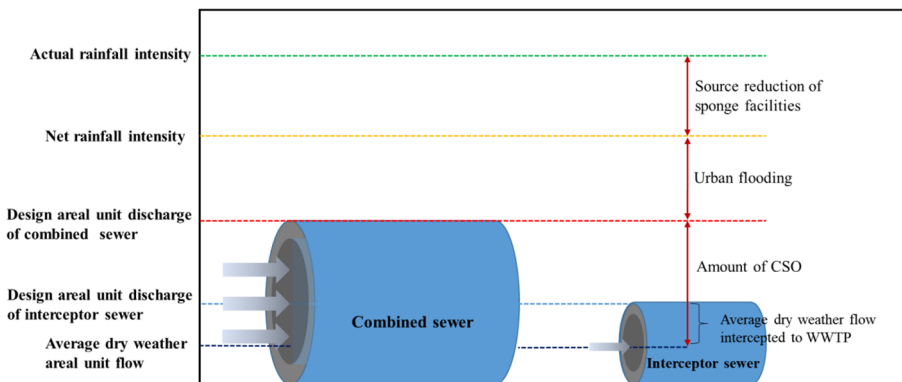


Fig. 2 Principle of excess rainfall intensity of double thresholds (ERI_d)

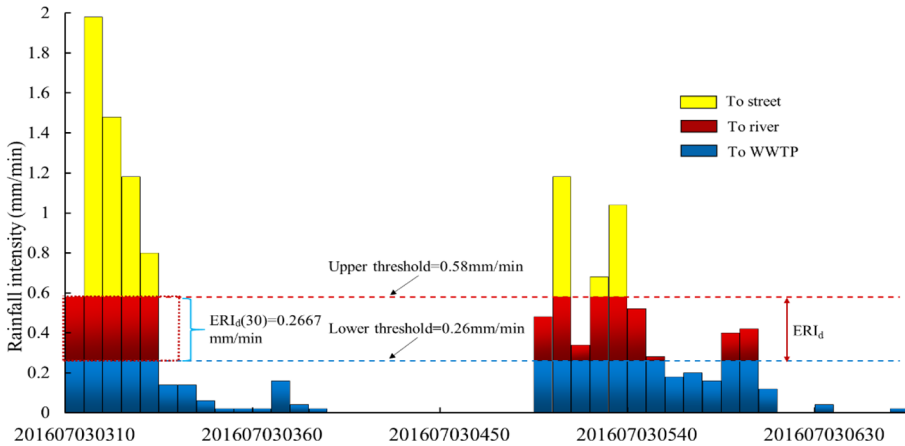


Fig. 3 Calculation of ERI_d for the single rainfall event

According to Fig. 3, the total excess rainfall intensity (ERI) and the corresponding total CSO duration for the single rainfall event can be obtained. Normally, the specific CSO duration can be selected for calculation of ERI_d . Thus, ERI_d equals to the total ERI during the specific duration divided by this duration. It can be expressed as $ERI_{d(CSO\ duration)}$. In this study, 30-minute CSO duration was illustrated for calculation of $ERI_{d(30)}$.

After ERI_d calculation for the single rainfall event, a number of ERI_d samples can be collected annually. Similar to rainfall intensity sampling for storm sewer design, annual maxima sampling (AMS) method and annual multiple sampling method can be used here. In order to focus on studying the frequency distribution characteristics of ERI, all ERI samples of rainfall events were used for subsequent frequency calculations in this work.

2.3 Calculation of the Empirical Frequency of ERI_d

All the samples of ERI_d are sorted in the descending order, and their corresponding empirical frequency can be calculated according to the mathematical expectation formula or Weibull formula (Weibull 1939), as shown below:

$$P = \frac{m}{n + 1} \times 100\% \tag{2}$$

where P is the empirical frequency, m is the serial number and n is the amount of samples.

2.4 Selection of Frequency Distribution for ERI_d

According to the double-threshold characteristics of ERI_d , its frequency distribution can be modeled by the doubly censored distribution theory. In this study, this theory is based on that the main part of the CSO is a distribution truncated at both ends between the lower threshold value d and the upper threshold value u , i.e., the population distribution of ERI_d is the conditional distribution of the $[d, u]$ part. Assuming that $F(x, \theta)$ is the distribution func-

tion of ERI_d and $f(x, \theta)$ is the corresponding probability density function, θ is a parameter that can be estimated using optimization algorithm. The doubly censored distribution function and density function are shown in Eq. (3) and Eq. (4) (Chen 2019; Tian et al. 2014):

$$F(x; \theta | d \leq x \leq u) = \frac{F(x, \theta) - F(d, \theta)}{F(u, \theta) - F(d, \theta)} \quad (3)$$

$$f(x; \theta | d \leq x \leq u) = \frac{f(x, \theta)}{F(u, \theta) - F(d, \theta)} \quad (4)$$

The conventional doubly censored distribution can be calculated from the Eq. (3) and Eq. (4). The density functions of normal and exponential distributions under doubly censored conditions are given in similar computational studies as shown in Eq. (5) and Eq. (6).

Doubly censored normal distribution:

$$f(x | d \leq x \leq u) = \frac{1}{[\varphi(\frac{u-\mu}{\sigma}) - \varphi(\frac{d-\mu}{\sigma})\sqrt{2\pi}\sigma] \exp[-\frac{(x-\mu)^2}{2\sigma^2}]} \quad (5)$$

Doubly censored exponential distribution:

$$f(x | d \leq x \leq u) = \frac{\lambda e^{-\lambda x}}{e^{-\lambda d} - e^{-\lambda u}} \quad (6)$$

where d is the lower threshold parameter; u is the upper threshold parameter; μ represents the average value; σ represents the standard deviation; ϕ is the cumulative distribution of the standard normal distribution.; λ is the parameter and is estimated by MCMC algorithm in this study.

In addition, several probability density distribution functions were also investigated in this study to analyze the frequency distribution characteristics of the ERI_d , such as lognormal, exponential, Gumbel, and Weibull distributions (Ahmad I 2019; Alhassoun 2011; Haddad et al. 2011; Yilmaz et al. 2014). The coefficient of determination R^2 is a commonly used goodness-of-fit statistic in regression analysis to assess fitting performance (Fu et al. 2014). In this work, it was used to evaluate the accuracy of model fitting.

2.5 Study data

In this study, a set of ten-year recorded rainfall series (2008/01/01 to 2017/12/31) from a meteorological station in Sichuan Province, southwestern China, was used for illustration, its temporal resolution is 5 min, as shown in Fig. 4.

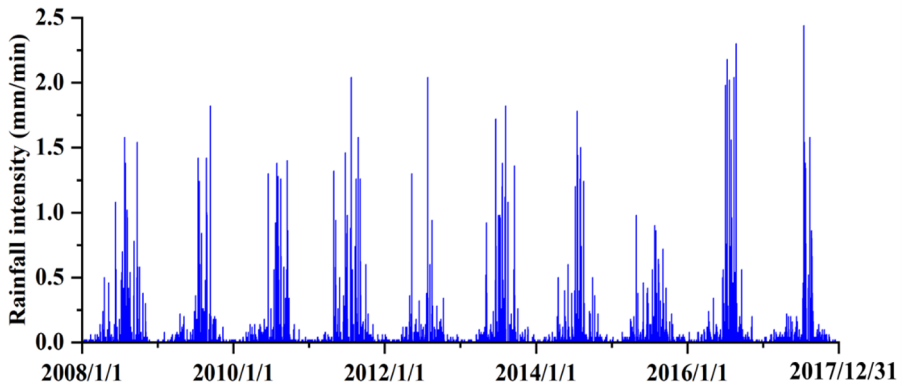


Fig. 4 The recorded rainfall series for the case study (2008/01/01-2017/12/31)

Table 1 Statistics of rainfall events

Year	Amount of rainfall events	Maximum duration (minute)	Average duration (minute)	Maximum rainfall depth (mm)	Average rainfall depth (mm)	Maximum rainfall intensity (mm/min)	Average rainfall intensity (mm/min)
2008	70	1810	436.36	82.2	14.21	1.58	0.03
2009	56	2345	443.13	66.1	12.13	1.82	0.03
2010	74	1635	392.64	96.7	12.18	1.40	0.03
2011	64	1165	458.05	83.3	14.85	2.04	0.03
2012	66	1725	440.98	44.2	8.61	2.04	0.02
2013	77	4015	403.70	322.9	16.72	1.82	0.04
2014	62	1870	427.02	105	13.85	1.78	0.03
2015	68	2475	431.10	156.9	12.10	0.98	0.03
2016	70	1910	429.86	79.9	13.19	2.30	0.03
2017	87	1085	371.32	108.4	10.37	2.44	0.03
Total(2008–2017)	694	20,035	4234.15	1145.6	128.20	18.20	0.30
Average	69.4	2003.5	423.41	114.56	12.82	1.82	0.03

3 Results and Discussions

3.1 Statistical Results of Rainfall Event Division

For MIET=3 h, the original rainfall series were divided into 694 single rainfall events. The statistics of rainfall events were shown in Table 1.

3.2 Sampling Results of ERI_d

In this study, eight sets of double-threshold scenarios ([0.26,0.58], [0.33,0.76], [0.40,0.91], [0.49,1.11], [0.58,1.32], [0.65,1.46], [0.73,1.65], [0.83,1.88] mm/min) were used for sampling ERI_d for all the above rainfall events. These upper and lower thresholds were calculated according to the corresponding rainfall intensity formula under the specific return

period. Moreover, taking CSO duration of 30 min as an example, the results of $ERI_{d(30)}$ for the representative rainfall event (3:10 2008/7/3 to 6:50 2008/7/3) were shown in Table 2. Among them, the maximum of $ERI_{d(30)}$ was sampled for the specific rainfall event (only sample one maximum of ERI_d for a rainfall event), as shown in Fig. 3. The sampling results of $ERI_{d(30)}$ were shown in Table 3.

It was found that from Table 3: (1) The average values of $ERI_{d(30)}$ are all larger than the median value, and C_s for all scenarios are larger than zero, which indicate that the frequency distribution of ERI_d is right-skewed. (2) The average values of C_v of $ERI_{d(30)}$ under different double thresholds is almost 1, which shows that the ERI_d samples are less discrete. (3) None of the kurtosis is greater than 3, which indicates that the frequency distribution of $ERI_{d(30)}$ is thin-tailed.

3.3 Results for Empirical Frequency of $ERI_{d(30)}$

The empirical frequencies of the $ERI_{d(30)}$ samples were calculated using Eq. (2). Part of the empirical frequency results of $ERI_{d(30)}$ for the double thresholds [0.26,0.58] were shown in Table 4. The curves of the empirical frequency distribution of $ERI_{d(30)}$ for different double-threshold scenarios were shown in Fig. 5. It can be found that the empirical frequency distributions of $ERI_{d(30)}$ samples have the similar tendency in different double-threshold scenarios.

3.4 Results of the “theoretical” Frequency Distribution

In this study, doubly censored exponential distribution, exponential function, Gumbel distribution, Weibull distribution, and lognormal distribution were selected to fit frequency distribution function of $ERI_{d(30)}$. Meanwhile, MCMC algorithm was used to estimate parameters of the above distributions (Liu et al. 2021). Results of parameter optimization were shown in Table 5, and results of the doubly censored exponential distribution were shown in Fig. 6. The comparison of the frequency of fitting each function to ERI_d was shown in Table 6. It reveals that the doubly censored exponential distribution and the exponential distribution are suitable for characterizing ERI_d and the Gumbel, Weibull, and lognormal distributions are not suitable for ERI_d . Among them, the doubly censored exponential distribution is the best theoretical frequency distribution for ERI_d .

3.5 Discussions

In this work, the method for calculating the frequency distribution of ERI_d was proposed based on the double-threshold occurrence mechanism of CSO. It provides a relatively universal method for predicting the severity of CSO from the specific interceptor well based on the recorded rainfall series. For this method, two critical parameters are needed: the areal unit flow rate of the upstream combined sewer and the downstream interceptor sewer. Generally, they can be obtained from the original design archives of the combined sewer system or the on site measurement.

In addition, the net rainfall process (including depression and infiltration) was temporarily neglected in this study. Normally, it only has impacts on the initial stage of rainfall-runoff process of the tributary catchments and the most intense rainfall process seldom occurs in

Table 2 Results of ERI_d for the typical rainfall event

Time	Actual rainfall intensity (mm/min)	lower threshold (mm/min)	upper threshold (mm/min)	$ERI_{d(5)}$ (mm/min)	$ERI_{d(30)}$ (mm/min)
201,607,030,310	0.58	0.26	0.58	0.32	0.2667
201,607,030,315	1.98	0.26	0.58	0.32	0.2133
201,607,030,320	1.48	0.26	0.58	0.32	0.1600
201,607,030,325	1.18	0.26	0.58	0.32	0.1067
201,607,030,330	0.8	0.26	0.58	0.32	0.0533
201,607,030,335	0.14	0.26	0.58	0.00	0.0000
201,607,030,340	0.14	0.26	0.58	0.00	0.0000
201,607,030,345	0.06	0.26	0.58	0.00	0.0000
201,607,030,350	0.02	0.26	0.58	0.00	0.0000
201,607,030,355	0.02	0.26	0.58	0.00	0.0000
201,607,030,360	0.02	0.26	0.58	0.00	0.0000
201,607,030,405	0.16	0.26	0.58	0.00	0.0000
201,607,030,410	0.04	0.26	0.58	0.00	0.0000
201,607,030,415	0.02	0.26	0.58	0.00	0.0000
201,607,030,420	0	0.26	0.58	0.00	0.0000
201,607,030,425	0	0.26	0.58	0.00	0.0000
201,607,030,430	0	0.26	0.58	0.00	0.0000
201,607,030,435	0	0.26	0.58	0.00	0.0000
201,607,030,440	0	0.26	0.58	0.00	0.0000
201,607,030,445	0	0.26	0.58	0.00	0.0000
201,607,030,450	0	0.26	0.58	0.00	0.0367
201,607,030,455	0	0.26	0.58	0.00	0.0900
201,607,030,460	0	0.26	0.58	0.00	0.1033
201,607,030,505	0	0.26	0.58	0.00	0.1567
201,607,030,510	0	0.26	0.58	0.00	0.2100
201,607,030,515	0.48	0.26	0.58	0.22	0.2533
201,607,030,520	1.18	0.26	0.58	0.32	0.2200
201,607,030,525	0.34	0.26	0.58	0.08	0.1667
201,607,030,530	0.68	0.26	0.58	0.32	0.1533
201,607,030,535	1.04	0.26	0.58	0.32	0.1000
201,607,030,540	0.52	0.26	0.58	0.26	0.0700
201,607,030,545	0.28	0.26	0.58	0.02	0.0533
201,607,030,550	0.18	0.26	0.58	0.00	0.0500
201,607,030,555	0.2	0.26	0.58	0.00	0.0500
201,607,030,560	0.16	0.26	0.58	0.00	0.0500
201,607,030,605	0.4	0.26	0.58	0.14	0.0500
201,607,030,610	0.42	0.26	0.58	0.16	0.0267
201,607,030,615	0.12	0.26	0.58	0.00	0.0000
201,607,030,620	0	0.26	0.58	0.00	0.0000
201,607,030,625	0	0.26	0.58	0.00	0.0000
201,607,030,630	0.04	0.26	0.58	0.00	0.0000
201,607,030,635	0	0.26	0.58	0.00	0.0000
201,607,030,640	0	0.26	0.58	0.00	0.0000
201,607,030,645	0	0.26	0.58	0.00	0.0000
201,607,030,650	0.02	0.26	0.58	0.00	0.0000

Table 3 Sampling results for $ERI_{d(30)}$

Thresholds (min/min)	[0.26, 0.58]	[0.33, 0.76]	[0.40, 0.91]	[0.49, 1.11]	[0.58, 1.32]	[0.65, 1.46]	[0.73, 1.45]	[0.83, 1.88]
Number of samples	196	178	141	123	96	88	85	72
Average value (mm/min)	0.12	0.13	0.16	0.17	0.19	0.18	0.17	0.16
Standard deviation	0.10	0.13	0.15	0.17	0.18	0.19	0.19	0.18
Median value (mm/min)	0.08	0.08	0.11	0.11	0.12	0.11	0.09	0.08
Cv	0.87	1.01	0.96	1.03	0.97	1.00	1.13	1.15
Cs	3.06	3.53	3.36	3.61	3.39	3.51	3.95	4.04
Kurtosis	-0.76	-0.30	-0.11	0.42	0.76	1.31	2.26	3.00

Table 4 Empirical frequency of ERI_d samples

No.	$ERI_{d(30)}$ (mm/min)	The empirical frequency (%)
1	0.344	0.51
2	0.343	1.02
3	0.341	1.52
...
17	0.313	8.63
...
196	0.0033	99.49

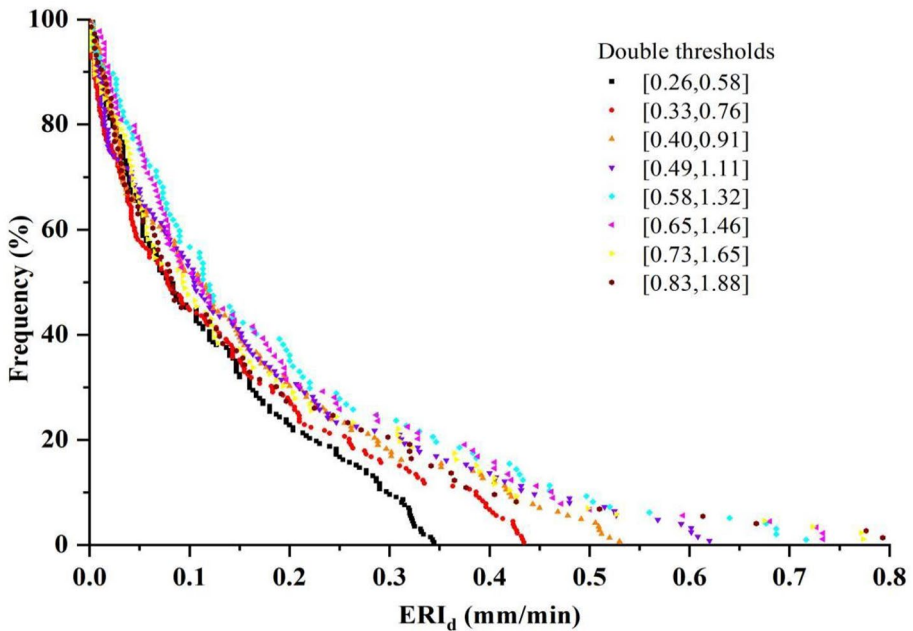


Fig. 5 The empirical frequency of the ERI_d sample data

Table 5 Parameter optimization results for doubly censored exponential distribution

Thresholds (mm/min)	λ
[0.26,0.58]	9.0536
[0.33,0.76]	7.4771
[0.40,0.91]	6.6116
[0.49,1.11]	5.6296
[0.58,1.32]	5.0518
[0.65,1.46]	4.5889
[0.73,1.65]	4.1043
[0.83,1.88]	3.6947

Note: The dots in the figure represent empirical frequency and the lines represent theoretical frequency

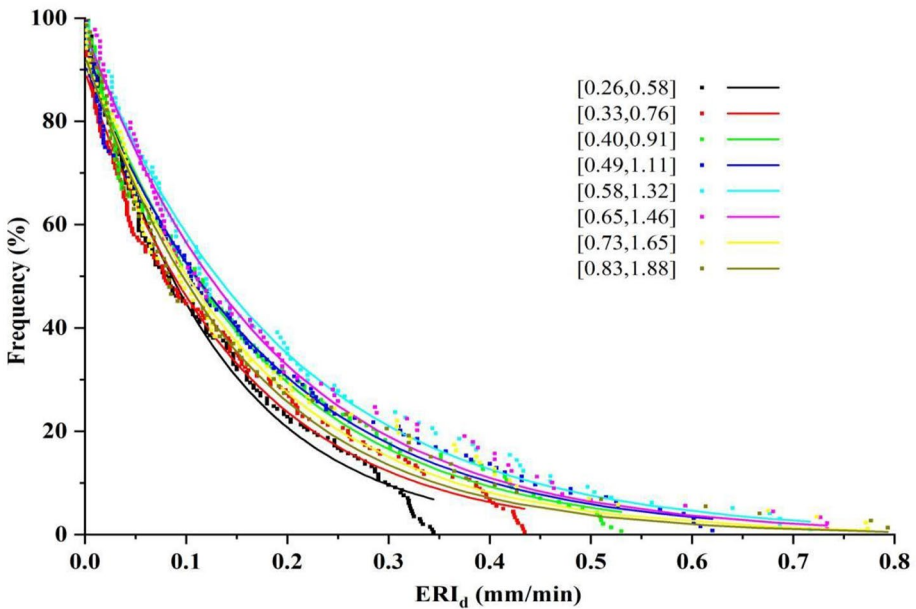


Fig. 6 Comparison of the empirical and the theoretical frequency distribution of $ERI_{d(30)}$

Table 6 Comparison of the fitting performance for frequency distribution of $ERI_{d(30)}$

Thresholds (min/min)	R^2								Mean value
	[0.26, 0.58]	[0.33, 0.76]	[0.40, 0.91]	[0.49, 1.11]	[0.58, 1.32]	[0.65, 1.46]	[0.73, 1.45]	[0.83, 1.88]	
Doubly censored exponential	0.9984	0.9968	0.9975	0.9979	0.9989	0.9958	0.9888	0.9811	0.9944
Exponential	0.9922	0.9857	0.9880	0.9908	0.9957	0.9916	0.9896	0.9875	0.9901
Gumbel	The fit does not converge								
Weibull	The fit does not converge								
Lognormal	The fit does not converge								

the early stages of rainfall event. Meanwhile, if more accurate results are expected to get, the actual dry weather flow of the combined sewer system should also be measured.

Moreover, the resulted frequency distribution of ERI_d (e.g. the doubly censored exponential distribution and the exponential distribution in this work) are site specific. Particularly, it is related to the rainfall data used, the situations of sewer linking the interceptor well, etc. Therefore, more attention should be paid to demonstrate this result in the future research.

Finally, this work is very helpful for evaluating or even predicting CSO behaviour for the specific interceptor well. Based on the frequency distribution of ERI_d derived from this method and the corresponding CSO duration, the volume of CSO can be calculated under certain frequency conditions, which is useful for rationally design CSO abatement and treatment facilities.

4 Conclusions

In this study, a double-threshold method of excess rainfall intensity (ERI_d) was proposed for characterizing CSO. For the specific interceptor well, the upper threshold is the design areal unit discharge (the equivalent rainfall intensity) of its upstream combined sewer and the lower one is the design areal unit discharge of its downstream interceptor sewers minus dry weather flow rate. In addition, the frequency distribution of ERI_d was initially investigated. Finally, a case study was conducted based on a 10-year rainfall time series. Eight sets of double thresholds ([0.26,0.58], [0.33,0.76], [0.40,0.91], [0.49,1.11], [0.58,1.32], [0.65,1.46], [0.73,1.65], [0.83,1.88] mm/min) and one typical CSO durations (30 min) were demonstrated. The results showed that: (1) The excess rainfall intensity of double thresholds (ERI_d) is suitable for characterizing CSO. (2) The frequency distribution of ERI_d was right (positively) skewed based on the statistics of ERI_d samples. (3) The kurtosis of the ERI_d samples is not greater than 3 for all the thresholds studied, which indicates that the distribution is thin-tailed. (4) In this study, the optimal frequency distribution function for ERI_d is doubly censored exponential distribution.

Author Contributions Xingpo Liu designed the study, co-wrote the the initial draft of the manuscript, Writing-review and Editing. Liang Shen performed the research and co-wrote the initial draft of the manuscript, Writing-review and Editing. Wenke Zang performed the research and co-wrote the initial draft of the manuscript. Yuwen Zhou contributed to the roadmap of the study.

Funding This study was supported by the National Natural Science Foundation of China [Grant No. 51008191].

Data Availability The authors confirm that some data are available from the corresponding author on reasonable request.

Declarations

Ethics Approval This paper has neither been published nor been under review for publication elsewhere.

Consent to Participate The authors have participated in the preparation of this paper for publication in the Water Resources Management.

Consent to Publish The authors declare their consent to publication of the manuscript in “Water Resources Management” journal.

Competing Interests Authors declare no conflict of interest.

References


- Ahmad I, Khan D, Almanjahie IM et al (2019) At-Site rainfall frequency analysis using partial duration series and annual maximum series: a case study. *Ecol Appl* 17(4):8351–8367. https://doi.org/10.15666/acer/1704_83518367
- Alhassoun SA (2011) Developing an empirical formulae to estimate rainfall intensity in Riyadh region. *J King Saud Univ Eng Sci* 23(2):81–88. <https://doi.org/10.1016/j.jksues.2011.03.003>
- Andrés-Doménech I, Múnera JC, Francés F, Marco JB (2010) Coupling urban event-based and catchment continuous modelling for combined sewer overflow river impact assessment. *Hydrol Earth Syst Sci* 14(10):2057–2072. <https://doi.org/10.5194/hess-14-2057-2010>
- Atauzzaman M, Ali MA (2022) Effects of combined sewer overflow on water quality: a case study of Hatirjheel Lake in Dhaka. *SN Appl Sci* 4(11):303. <https://doi.org/10.1007/s42452-022-05187-6>
- Bizer AM, Kirchoff CJ (2022) Regression modeling of combined sewer overflows to assess system performance. *Water Sci Technol* 86(11):2848–2860. <https://doi.org/10.2166/wst.2022.362>
- Campisano A, Creaco E, Modica C (2016) Application of Real-Time Control Techniques to Reduce Water volume discharges from Quality-oriented CSO devices. *J Environ Eng* 142(1):04015049. [https://doi.org/10.1061/\(ASCE\)EE.1943-7870.0001013](https://doi.org/10.1061/(ASCE)EE.1943-7870.0001013)
- Chen Q (2019) Piecewise-defined severity distribution Approach of operational risk based on Truncated Data and Its application. *J Syst Manag* 28(05):907–916. <https://doi.org/10.3969/j.issn.1005-2542.2019.05.013>(in Chinese)
- Dai LF, Du S, Lin XJ et al (2020) Study on Overflow Frequency Control Rate of Overflow Pollution Control Standard in Urban Combined Sewer System. *China Water Wastewater* 36(12):56–59. <https://doi.org/10.19853/j.zgjssps.1000-4602.2020.12.010>(in Chinese)
- Fortier C, Mailhot A (2015) Climate Change Impact on Combined Sewer overflows. *J Water Resour Plan Manag* 141(5):04014073. [https://doi.org/10.1061/\(ASCE\)WR.1943-5452.0000468](https://doi.org/10.1061/(ASCE)WR.1943-5452.0000468)
- Fu C, Wang KJ (2024) LASSO Regression assisted by coefficient of determination and correlation coefficient. *J Fujian Norm Univ Nat Sci Ed* 40(02):57–63 (in Chinese)
- Guan GL, Fu R, Li P (2023) Practice and thinking on comprehensive management of urban river water environment. *Water Resour Plann Des* 05:80–85 (in Chinese)
- Haddad K, Rahman A (2011) Selection of the best fit flood frequency distribution and parameter estimation procedure: a case study for Tasmania in Australia. *Stoch Environ Res Risk Assess* 25(3):415–428. <https://doi.org/10.1007/s00477-010-0412-1>
- Li JQ, Zhou JC, Yang Z (2021) Study on control indicators and standard formulation of combined sewer overflow. *Water Resour Prot* 37(01):124–131. <https://doi.org/10.3880/j.issn.1004-6933.2021.01.018>(in Chinese)
- Liu XP, Xia CF, Tang YF, Tu JY, Wang HM (2021) Parameter optimization and uncertainty assessment for rainfall frequency modeling using an adaptive metropolis–Hastings algorithm. *Water Sci Technol* 83(5):1085–1102. <https://doi.org/10.2166/wst.2021.032>
- Liu XP, Ouyang CM, Zhou YW (2023) A low-return-period rainfall intensity formula for estimating the design return period of the combined Interceptor sewers. *Water Resour Manag* 37(1):289–304. <https://doi.org/10.1007/s11269-022-03369-w>
- Liu XP, Zang WK, Zhou YW (2024) A Method for estimating excess rainfall intensity (ERI) of combined sewer overflow (CSO) based on peak over threshold (POT) sampling and the generalized pareto distribution (GPD). *Water Resour Manag* 38(3):1045–1060. <https://doi.org/10.1007/s11269-023-03708-5>
- Mailhot A, Talbot G, Lavallée B (2015) Relationships between rainfall and combined Sewer Overflow (CSO) occurrences. *J Hydrol* 523:602–609. <https://doi.org/10.1016/j.jhydrol.2015.01.063>
- Pu GB, Xie T, Shao C (2022) Confusion and suggestions on Pollution Control of Sewage Overflow in Chongqing Municipality. *China Water Wastewater* 38(18):1–5. <https://doi.org/10.19853/j.zgjssps.1000-4602.2022.18.001>(in Chinese)
- Quaranta E, Fuchs S, Liefing HJ, Schellart A, Pistocchi A (2022) A hydrological model to estimate pollution from combined sewer overflows at the regional scale: application to Europe. *J Hydrol-Reg Stud* 41:101080. <https://doi.org/10.1016/j.ejrh.2022.101080>

- Salam A (2024) Stormwater Management modeling (SWMM). *Internet Things Smart Sewer Drain Syst* 51–59. <https://doi.org/10.1007/978-3-031-48109-3>
- Schroeder K, Riechel M, Matzinger A, Rouault P, Sonnenberg H, Pawlowsky-Reusing E, Gnirss R (2011) Evaluation of effectiveness of combined sewer overflow control measures by operational data. *Water Sci Technol* 63(2):325–330. <https://doi.org/10.2166/wst.2011.058>
- Tian RJ, Tian XJ, Li JL (2014) Fitting research on ship's oil spill loss based on DTD-GPD distribution. *Port Waterw Eng* 0341–44. <https://doi.org/10.16233/j.cnki.issn1002-4972.2014.03.005> (in Chinese)
- Wang Q, Quan CL (2020) Study on combined system overflow pollution control planning of Beijing Longtan West Lake area based on mathematical model. *Water Wastewater Eng* 56(11):54–59. <https://doi.org/10.13789/j.cnki.wwe1964.2020.11.010> (in Chinese)
- Weibull W (1939) A statistical theory of the strength of materials. *Stockh: Ingeniors Vetensk Acad Handl*:1–45
- Yilmaz AG, Safaet H, Huang F, Perera BJC (2014) Time-varying character of storm intensity frequency and duration curves. *Australas J Water Resour* 18(1):15–26. <https://doi.org/10.7158/W12-017.2014.18.1>
- Yu Y, Kojima K, An K, Furumai H (2013) Cluster analysis for characterization of rainfalls and CSO behaviours in an urban drainage area of Tokyo. *Water Sci Technol* 68(3):544–551. <https://doi.org/10.2166/wst.2013.253>
- Yu Y, Zhang SZ, An AK, Furumai H (2018) Simple method for calculating hydraulic behavior of combined sewer overflow from Rainfall Event Data. *J Water Resour Plan Manag* 144(10):04018061. [https://doi.org/10.1061/\(ASCE\)WR.1943-5452.0000972](https://doi.org/10.1061/(ASCE)WR.1943-5452.0000972)
- Zhang C, Ma XL, Lu F, Li P (2016) Code for design of outdoor wastewater engineering (GB 50014). China Plan, Beijing, pp 1–248. (in Chinese)

Publisher's Note Springer Nature remains neutral with regard to jurisdictional claims in published maps and institutional affiliations.

Springer Nature or its licensor (e.g. a society or other partner) holds exclusive rights to this article under a publishing agreement with the author(s) or other rightsholder(s); author self-archiving of the accepted manuscript version of this article is solely governed by the terms of such publishing agreement and applicable law.

Authors and Affiliations

Xingpo Liu¹  · Liang Shen¹ · Wenke Zang¹ · Yuwen Zhou²

✉ Xingpo Liu
stormmodel@163.com

¹ College of Ocean Science and Engineering, Shanghai Maritime University, Shanghai 201306, P.R. China

² College of Architectural and Civil engineering, Beijing University of Technology, Beijing 100124, P.R. China